New NiO/Co_3O_4 and Fe_2O_3/Co_3O_4 Nanocomposite Catalysts: Synthesis and Characterization

Marta Maria Natile and Antonella Glisenti*

Dipartimento di Chimica Inorganica, Metallorganica ed Analitica, Università di Padova, via Loredan, 4-35131 Padova, Italy

Received January 17, 2003. Revised Manuscript Received March 21, 2003

Two nanocomposite oxides, NiO/Co_3O_4 and Fe_2O_3/Co_3O_4, are considered. The nanocomposite oxides were obtained by wet impregnation and characterized by means of X-ray photoelectron spectroscopy (XPS), diffuse reflectance infrared Fourier transform (DRIFT) spectroscopy, X-ray diffraction (XRD), thermal analysis, atomic force microscopy (AFM), and transmission electron microscopy (TEM). The microscopy images suggest a different growing mechanism for the NiO/Co_3O_4 and Fe_2O_3/Co_3O_4 nanocomposite oxides: small clusters of iron oxide wet the surface of Co_3O_4, whereas NiO grows as isolated particles characterized by a big diameter. Both XPS and TEM data indicate the possible formation of Fe_3O_4. A marked decrease of OH groups on the Fe_2O_3/Co_3O_4 and NiO/Co_3O_4 sample surfaces is revealed by XPS and DRIFT data and suggests the grafting of supported and supporting oxides by hydroxyl condensation. The acidic and basic sites present on Fe_2O_3/Co_3O_4 and NiO/Co_3O_4 powder surfaces are investigated and compared with those observed on the Co_3O_4 oxide. New Lewis and Brønsted acidic sites are observed on the Fe_2O_3/Co_3O_4 sample, whereas the complex sites constituted by a cation and its neighboring oxygen atom (observed on the iron oxide surface) disappear. In the NiO/Co_3O_4 mixed oxide sample, new acidic/basic sites were never revealed. The Fe_2O_3/Co_3O_4 supported oxide influences the stability of the Co_3O_4 with respect to its reduction to CoO.

Introduction

Transition metal oxides are getting more and more important in several fields of materials technology. Their importance in applied catalysis or in energy conversion, for example, does not need to be underlined. This importance justifies studies aiming for better comprehension of the surface reactivity of metal oxides. In fact, investigation of the interaction mechanisms and reaction paths as a function of the surface acidic/basic sites can be useful to reach a better comprehension and to accordingly design new materials. In this respect, mixed oxides offer great possibilities for allowing tuning of the properties of the materials. New active acid/base or redox sites can be obtained by mixing different components (different metals), by choosing an adequate preparation procedure, or with specific posttreatments. Particularly interesting are the nanocomposite materials prepared by depositing an active oxide on a supporting one. Wet impregnation allows deposition of small clusters of active oxide on the support taking advantage of the particular reactivity offered by the very small dimensions. Moreover, an active oxide may be used as a support and new acidic/basic or redox sites, different from those observed on the pure oxide surfaces, can be obtained.

In this paper we focus our attention on two supported metal oxides obtained by wet impregnation. The investigated systems were obtained by supporting NiO and Fe_2O_3 on Co_3O_4. The reactivity with respect to methanol will be also considered,[1] whereas the reactivity of the pure oxides powders was already investigated.[2−4]

The nanocomposite nature of the samples was hypothesized following the XPS results and confirmed by means of TEM images; further information concerning the growing mode can also be derived from AFM and TEM images. Besides the morphological characterization, the nanocomposite oxide samples were investigated with the aim of understanding the surface acidic/basic sites; the obtained results were compared with those observed on the pure oxides. It is well-known[5,6] that pyridine can interact with Lewis and Brønsted acidic sites distributed on the oxide surface giving rise to different adsorbed species. Their characterization allows distinction among different acid sites. CO_2 is preferred for the investigation of the Lewis base sites.[6]

It is noteworthy that the acidic/basic sites investigation was carried out with avoiding any activation or cleaning treatment. The effect of the activation/cleaning

* Corresponding author. Fax: +39-049-827-5161. E-mail: glisenti@chin.unipd.it.

(1) Natile, M. M.; Glisenti, A. *Chem. Mater.*, submitted for publication.
(2) Natile, M. M.; Glisenti, A. *Chem. Mater.* **2002**, *14*, 4895.
(3) Natile, M. M.; Glisenti, A. *Chem. Mater.* **2002**, *14*, 3090.
(4) Glisenti, A.; Favero, G.; Granozzi, G. *J. Chem. Soc., Faraday Trans.* **1998**, *94*, 173.
(5) Kung, H. H. In *Transition Metal Oxides: Surface Chemistry and Catalysis*; Elsevier: Amsterdam, The Netherlands, 1989.
(6) Lahousse, C.; Aboulayt, A.; Maugé, F.; Bachelier, J.; Lavalley, J. C. *J. Mol. Catal.* **1993**, *84*, 283.

10.1021/cm031019e CCC: $25.00
Published on Web 05/31/2003

Table 1. XPS Peak Positions (BE in eV) Observed for the Supported Oxides, with Corresponding Values Obtained for the Pure Oxides and Literature Data Also Reported

sample	Ni2p$_{3/2}$	shake-up Ni 2p$_{3/2}$	Fe2p$_{3/2}$	shake-up Fe2p$_{3/2}$	Co2p$_{3/2}$	O1s(I)	O1s(II)	O1s(III)	Ni/Co	Fe/Co
NiO/Co$_3$O$_4$	854.0 855.4	861.4			780.1	529.6	531.5		0.1	
NiO[a]	854.4	861.5				529.6	531.3	533.4		
Ni(OH)$_2$[a]	855.6	862.8				530.9	532.9			
NiO[b]	854.6	861.7				529.7	531.4			
Fe$_2$O$_3$/Co$_3$O$_4$			711.3	718.9	780.4	530.1	531.4	533.1		0.1
Fe$_2$O$_3$[c]			711.0	719.2		530.0	531.6			
Fe$_2$O$_3$[d,e]			711.2	719.0		530.0				
Co$_3$O$_4$[f]					780.3	530.0	531.2	533.0		

[a] Ref 2. [b] Ref 11. [c] This work. [d] Ref 12. [e] Ref 4. [f] Ref 3.

procedures on the surface reactivity will be the subject of following papers.

Experimental Section

(a) Catalysts Preparation. The catalysts were prepared by wet impregnation of dry Co_3O_4 powder. The Co_3O_4 was prepared as indicated elsewhere[3] and calcined at 573 K. The NiO/Co_3O_4 nanocomposite oxide was prepared by wet impregnation of the cobalt oxide powder with an aqueous solution containing increasing quantities of $Ni(NO_3)_2{\cdot}6H_2O$ [Ni/Co nominal atomic ratios 0.025; 0.050; 0.075; and 0.10]. The obtained suspension was maintained under stirring for 2 days and then kept at rest for 1 day. Water was then evaporated in air, and the obtained solid was dried at 573 K for 10 h and calcined in air for 30 h at 973 K.

The Fe_2O_3/Co_3O_4 nanocomposite oxide was prepared by wet impregnation of the cobalt oxide powder with an aqueous solution containing increasing quantities of $Fe(NO_3)_3{\cdot}9H_2O$ [Fe/Co nominal atomic ratios 0.025; 0.050; 0.075; 0.10; and 0.25]. The solid obtained after water evaporation was dried at 573 K for 10 h and calcined in air for 10 h at 773 K.

(b) Techniques. *XPS Measurements.* XPS spectra were recorded using a Perkin-Elmer PHI 5600 ci spectrometer with standard Al Kα and Mg Kα sources (1486.6 and 1253.6 eV, respectively) working at 350 W. The working pressure was less than 1×10^{-8} Pa. The spectrometer was calibrated by assuming the binding energy (BE) of the Au 4f$_{7/2}$ line to lie at 84.0 eV with respect to the Fermi level. Extended spectra (survey) were collected in the range 0−1350 eV (187.85 eV pass energy, 0.4 eV step, 0.05 s·step^{-1}). Detailed spectra were recorded for the following regions: C 1s, O 1s, Ni 2p, and Co 2p (11.75 eV pass energy, 0.1 eV step, 0.1 s·step^{-1}) for the sample NiO/Co_3O_4, and C 1s, O 1s, Fe 2p, and Co 2p (23.5 eV pass energy, 0.1 eV step, 0.1 s·step^{-1}) for the sample Fe_2O_3/Co_3O_4. The standard deviation in the BE values of the XPS line is 0.10 eV. The atomic percentage, after a Shirley type background subtraction,[7] was evaluated using the PHI sensitivity factors.[8] To account for charging problems, the C 1s peak was considered to be located at 285.0 eV, and the peak BE differences were evaluated.

The samples for the XPS measures were processed as a pellet by pressing the catalyst powder at ca. 7×10^6 Pa for 10 min. Prior to the XP analysis the pellets were evacuated at 1×10^{-3} Pa for 12 h.

XRD Measurements. XRD patterns were obtained with a Philips diffractometer with Bragg−Brentano geometry using Cu Kα radiation (40 kV, 40 mA, $\lambda = 0.154$ nm).

DRIFT Measurements. IR spectra were obtained by means of a Bruker IFS 66 spectrometer working in diffuse reflectance mode and are displayed in Kubelka−Munk units.[9,10] The resolution of the spectra was 4 cm^{-1}. The sample temperature was measured through a thermocouple inserted into the sample holder directly in contact with the powder.

The powders used for DRIFT analysis were kept in nitrogen flow to eliminate water traces until a stable IR spectrum was obtained.

Thermal Analysis. Thermogravimetric analysis (TGA) and differential scanning calorimetry (DSC) were carried out in a controlled atmosphere using the simultaneous differential techniques (SDT) 2960 of TA Instruments. Thermograms were recorded at 4 and 10 °C min^{-1} heating rates in air or nitrogen flow. The covered temperature ranged from RT to 1273 K.

AFM and TEM Measurements. Topographic AFM images of the catalyst were obtained on a Park Scientific Instruments (PSI) Autoprobe CP microscope using noncontact AFM in air at RT, adopting the constant force mode (the force being ca. 1−2 nN). The cantilever used was a PSI ultralever: a gold-coated silicon cantilever with a silicon tip (2 μm). The images are presented without any elaboration apart from background subtraction.

For transmission electron microscopy (TEM) observations a Philips 400T microscope operated at 120 keV was used. The microscope was equipped with an energy dispersive X-ray spectroscopy (EDXS) system with a C/U ultrathin window detector. Powder specimens were suspended in ethanol and spread onto a copper grid covered with an amorphous carbon film.

(c) Reaction Conditions. The pyridine used for the chemisorption was obtained from a commercial source (Sigma-Aldrich, spectroscopic grade) and used without further purification.

The exposure in the FTIR equipment has been done using the COLLECTOR apparatus for diffuse reflectance infrared Fourier transform (DRIFT) spectroscopy from Spectra-Tech, Inc. fitted with the HTHP (high-temperature/high-pressure) chamber. In the case of the chemisorption of pyridine, the HTHP chamber was filled with the vapors mixture flowing nitrogen through a bubbler containing the liquid; in the case of CO_2 (Air Liquide, 99.998%) the gas outlet was directly connected to the reaction chamber.

Results and Discussion

(a) Characterization. The nanocomposite oxide powder samples were characterized by means of XP and DRIFT spectroscopic techniques, XRD and thermal analysis, as well as AFM and TEM.

The XP peak positions obtained in both the supported oxides are summarized in Table 1 whereas the spectra are shown in Figures 1 and 2.

The XP Co 2p$_{3/2}$ peak positions (780.1 eV for NiO/Co_3O_4 and 780.4 eV for Fe_2O_3/Co_3O_4) agree, in both the supported systems, with the expected values for Co_3O_4

(7) Shirley, D. A. *Phys. Rev.* **1972**, *55*, 4709.
(8) Moulder, J. F.; Stickle, W. F.; Sobol, P. E.; Bomben, K. D. In *Handbook of X-ray Photoelectron Spectroscopy*; Chastain, J., Ed.; Physical Electronics: Eden Prairie, MN, 1992.
(9) Kubelka, P.; Munk, F. *Z. Tech. Phys.* **1931**, *12*, 593.
(10) Kortum, G. *Reflectance Spectroscopy*; Springer: New York, 1969.
(11) Roberts, M. W.; Smart, R., St. C. *Surf. Sci.* **1980**, *100*, 590.
(12) McIntyre, N. S.; Zetaruk, D. G. *Anal. Chem.* **1977**, *49*, 1521.

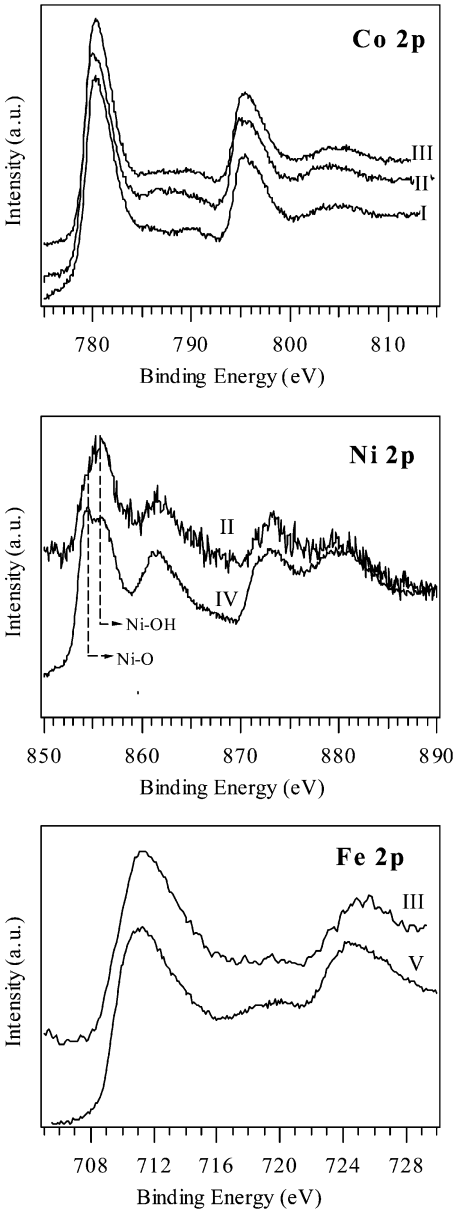

Figure 1. Co 2p, Ni 2p, and Fe 2p XPS spectra obtained on the supported oxide powders compared with the corresponding spectra of the pure oxides: (I) Co_3O_4, (II) NiO/Co_3O_4, (III) Fe_2O_3/Co_3O_4, (IV) NiO, and (V) Fe_2O_3. (The spectra are normalized with respect to their maximum value).

(780.3 eV);[3] the almost complete absence of the Co(II)shake-up peaks (at 787.0 and 804.0 eV) confirms this result.

The Ni $2p_{3/2}$ XP peak observed in NiO/Co_3O_4 shows two components at about 854.0 eV (Ni−O bonds) and 855.4 eV (Ni−OH bonds and multiplet splitting of the Ni−O peak); with respect to the NiO sample,[2] the contribution at 855.4 eV is prevalent suggesting a higher hydroxylation of NiO in the supported oxide surface. The O 1s peak confirms this result. The fitting procedure shows, for the NiO/Co_3O_4, two contributions at 529.6 and 531.5 eV, due to the M−O and M−OH bonds (M = Ni or Co), respectively. In the NiO/Co_3O_4 supported oxide the O 1s peak does not show the contribution around 533.0 eV (observed, in contrast, for NiO[2] and Co_3O_4[3]).

In the Fe_2O_3/Co_3O_4 supported oxide (Table 1) the Fe $2p_{3/2}$ peak position (711.3 eV) agrees with literature data

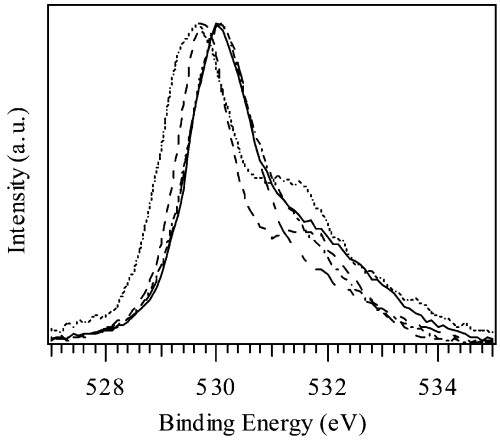

Figure 2. O 1s XPS spectra obtained on the supported oxide powders compared with the corresponding spectra observed for the pure oxides: (−) Co_3O_4, (- - -) NiO/Co_3O_4, (-·-·-·) Fe_2O_3/Co_3O_4, (···) NiO, and (− -) Fe_2O_3. (The spectra are normalized with respect to their maximum value).

Table 2. Nominal and Observed (XPS) Atomic Composition of the NiO/Co_3O_4 Supported Oxides

sample	nominal Ni/Co	XPS Ni/Co	XPS O/(Ni + Co)
NiO/Co_3O_4	0.025	0.06	1.39
	0.05	0.1	1.28
	0.075	0.15	1.56
	0.1	0.16	1.44

Table 3. Nominal and Observed (XPS) Atomic Composition of the Fe_2O_3/Co_3O_4 Supported Oxides

sample	nominal Fe/Co	XPS Fe/Co	XPS O/(Fe + Co)
Fe_2O_3/Co_3O_4	0.025	0.05	1.46
	0.05	0.1	1.44
	0.075	0.14	1.56
	0.1	0.185	1.52
	0.25	0.43	2.06

for Fe_2O_3.[4,12] The Fe(III) shake-up peak is observed at 718.9 eV.[13] The shake-up structure, however, is less evident than in pure Fe_2O_3 sample suggesting the partial reduction of the iron oxide particles. The O 1s peak shows three components at 530.1, 531.4, and 533.1 eV; the two contributions at lower BE are attributed to the M−O and M−OH bonds (M = Fe or Co), respectively, whereas the component at 533.1 eV suggests the presence of different M−OH bonds or chemisorbed water.

Ni/Co and Fe/Co XPS atomic ratios, obtained as a function of the nominal composition of the catalyst are summarized in Tables 2 and 3. Consistent with the surface-specific character of the XP spectroscopy and the preparation procedure, the obtained Ni/Co and Fe/Co atomic ratios are always higher than the corresponding nominal values (calculated from the weighted quantities). As a matter of fact, the wet impregnation procedure allows deposition of small particles on the surface of the supporting oxide. The supported oxides with atomic ratios Ni/Co = 0.1 (nominal composition Ni/Co = 0.05) and Fe/Co = 0.1 (nominal composition Fe/Co = 0.05) were selected for the adsorption experiments and further investigations.[14]

The XRD patterns (Figure 3) obtained for the nanocomposite oxide samples are very similar to the XRD

(13) Briggs, D.; Riviere, J. C. In *Practical Surface Analysis*; Briggs, D., Seah, M. P., Eds.; Wiley: New York, 1983.

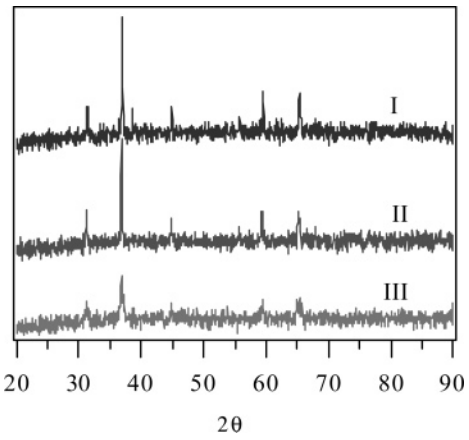

Figure 3. XRD spectra of the supported oxide compared with the spectrum obtained for Co_3O_4: (I) Co_3O_4, (II) NiO/Co_3O_4, and (III) Fe_2O_3/Co_3O_4.

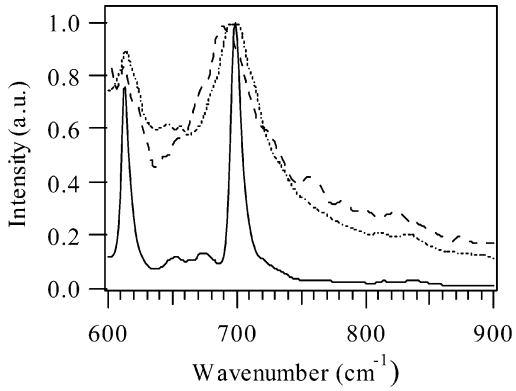

Figure 4. DRIFT spectra of the supported oxide catalysts compared with the corresponding spectrum of Co_3O_4, region between 600 and 900 cm^{-1}: (−) Co_3O_4, (···) NiO/Co_3O_4, and (- - -) Fe_2O_3/Co_3O_4.

pattern of Co_3O_4 and do not show contributions due to the iron or nickel oxides. This result can be due to the rather low Ni/Co and Fe/Co atomic ratios or to the low crystallinity of the deposited particles.

The Scherrer formula indicates that the average crystallite diameter is about 54 nm in the case of NiO/Co_3O_4 and 16 nm in the Fe_2O_3/Co_3O_4 system.[15] For this purpose the lower calcination temperature of the Fe_2O_3/Co_3O_4 (773 K for 10 h instead of the 973 K for 30 h of the NiO/Co_3O_4) nanocomposite oxide should be considered.

The DRIFT spectra of the supported oxides and of Co_3O_4[3] (Figure 4) are significantly different. In both the mixed oxide samples two very strong signals at 698 cm^{-1} and 612−613 cm^{-1} (Table 4), attributed to the longitudinal vibrations,[16,17] are evident. It is noteworthy that the longitudinal signals are very broad with respect to the corresponding peaks of Co_3O_4. This can be explained

Table 4. DRIFT Data (Wavenumbers cm^{-1}) Concerning the Longitudinal/Transversal Modes Observed for Co_3O_4 and for the Supported Oxides NiO/Co_3O_4 and Fe_2O_3/Co_3O_4

assignment	Co_3O_4	Co_3O_4[d]	NiO/Co_3O_4[e]	Fe_2O_3/Co_3O_4[e]
longitudinal modes	690[a]	698	698	698
	685[b]			
	683[c]			
longitudinal mode	605[a,b]	613	613	612
	619[c]			
transversal mode	660[a]			
	671[b]			
	683[c]			

[a] Ref 16. [b] Ref 17. [c] Ref 18. [d] Ref 3. [e] This work.

by taking into consideration that (1) the Ni−O and Fe−O bonds vibrations can contribute to the spectral region of low wavenumbers (less than 800 cm^{-1})[19] and (2) the interaction between the Co_3O_4 and the supported oxide can give rise to new Co sites with different chemical environments (Ni−O−Co or Fe−O−Co, for example).

The spectral region of the O−H stretching does not show significant peaks.

In contrast, the DRIFT spectrum of the Co_3O_4 powder sample[3] calcined at 573 K shows two signals at 3620 and 3550−3590 cm^{-1} attributed to OH groups and a broad band (3300−3500 cm^{-1}) due to the presence of water molecules. Hydroxyl groups are also evident on the surface of the α-Fe_2O_3 (3480, 3630−3635, 3649, 3675, 3690−3700, and 3720 cm^{-1})[4] and of the NiO (3619 and 3685 cm^{-1}) powder oxides.[2]

The marked decrease of OH groups observed on the NiO/Co_3O_4 and Fe_2O_3/Co_3O_4 sample surfaces and the shape of the longitudinal signals suggest the grafting of supported and supporting oxides by hydroxyl condensation.[20]

Thermal spectra are shown in Figure 5. The NiO/Co_3O_4 sample calcined at 573 K (Figure 5a) loses water gradually between RT and 792 K; the weight remains then constant until the Co_3O_4 decomposes to CoO at 1028 K. The Fe_2O_3/Co_3O_4 supported oxide (Figure 5b) loses water at temperatures lower than ca. 373 K and between 752 and 856 K. At 1063 K the cobalt oxide support decomposes to CoO. The weight loss of the samples calcined at temperatures higher than 573 K is very limited.

It is noteworthy that the presence of the iron oxide increases the Co_3O_4 decomposition temperature from ca. 1033 K (pure Co_3O_4) to 1063 K (Figure 5c). Moreover, with respect to the cobalt oxide, the weight loss of the Fe_2O_3/Co_3O_4 supported oxide is lower.

AFM images of the Fe_2O_3/Co_3O_4 and NiO/Co_3O_4 supported oxides are shown in Figure 6; comparison among the images clearly shows the formation of bigger particles in the NiO/Co_3O_4 supported oxide. Moreover, the particle dimensions seem to increase with the supported oxide concentration (Figure 6c), beyond the heat treatment.

(14) The Ni/Co and Fe/Co atomic ratios are related to the extent of surface coverage and suggest which samples expose both the supporting and the supported oxide. See, as an example, Argile, C.; Rhead, G. E. *Surf. Sci. Reports* **1989**, *10*, 277 and Fadley, C. S. In *Electron Spectroscopy: Theory, Techniques and Applications*; Brundle, C. R., Baker, A. D., Eds.; Academic Press, New York, 1978; Vol. 2, Chapter 1.

(15) Enzo, S.; Polizzi, S.; Benedetti, A. *Z. Kristall.* **1985**, *170*, 275.
(16) Nkeng, P.; Koenig, J.-F.; Gautier, J. L.; Chartier, P.; Poillerat, G. *J. Electroanal. Chem.* **1996**, *402*, 81.
(17) Shirai, H.; Morioka, Y.; Nakagawa I. *J. Phys. Soc. Jpn.* **1982**, *51*, 592.
(18) Lefez, B.; Nkeng, P.; Lopitaux, J.; Poillerat, G. *Mater. Res. Bull.* **1996**, *31*, 1263.
(19) Gielisse, P. J.; Plendl, J. N.; Mansur, L. C.; Marshall, R.; Mitra, S. S.; Mykolajewycz, R.; Smakula, A. *J. Appl. Phys.* **1965**, *36*, 2446.
(20) Schwarz, J. A.; Contescu, C.; Contescu, A. *Chem. Rev.* **1995**, *95*, 477.

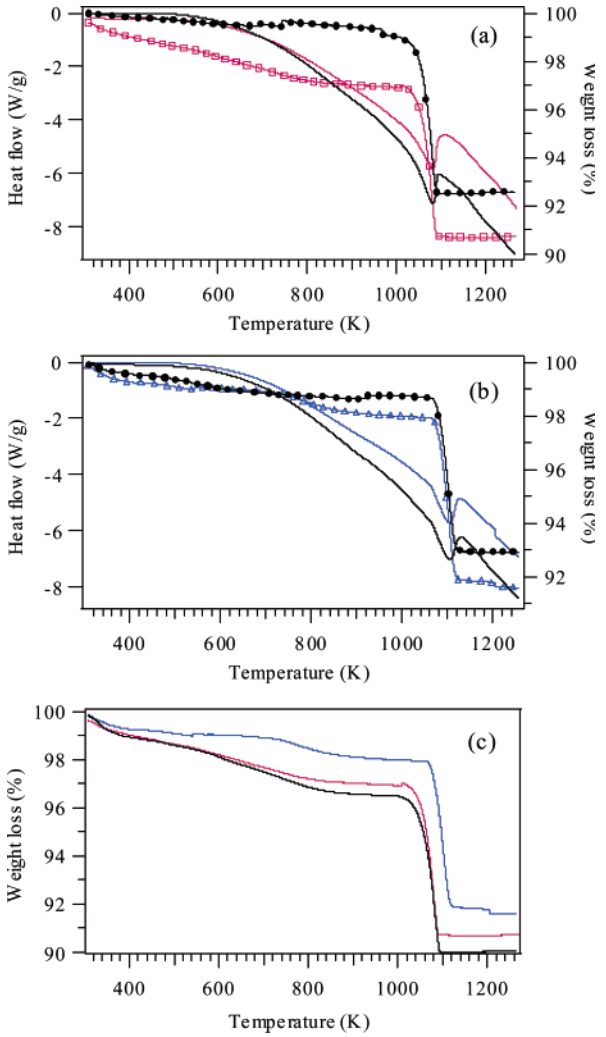

Figure 5. TGA and DSC (exotherm up) spectra (lines with and without markers, respectively) obtained on the supported oxide catalysts. (a) NiO/Co_3O_4 treated at 573 K (red) and at 973 K (black); (b) Fe_2O_3/Co_3O_4 treated at 573 K (blue) and at 773 K (black); (c) spectra of the supported oxide systems heated at 573 K compared with the spectrum (black) obtained for the Co_3O_4 powder (treated at 573 K).

Figure 7a and b shows the transmission electron microscopy images of the Fe_2O_3/Co_3O_4 supported oxides characterized by Fe/Co nominal atomic ratios of 0.05 and 0.25, respectively. The inspection of the images allows observation of the nano-dimensioned iron oxide particles grown on the cobalt oxide crystallite surfaces. The size of the iron oxide particles ranges from 3 to 9 nm with an average diameter of 5 nm. The EDXS analysis results, summarized in Table 5, suggest the possible formation of Fe_3O_4; this could explain the observed Fe 2p peak shape. It is noteworthy that in the sample characterized by a higher Fe/Co atomic ratio, the iron oxide particles tend to form bigger islands.

The TEM images of the NiO/Co_3O_4 supported oxide samples characterized by Ni/Co nominal atomic ratios of 0.05 and 0.1 are shown in Figure 8a and b, respectively; the images indicate the formation of a lower number of particles with respect to Fe_2O_3/Co_3O_4; moreover, these particles are characterized by a bigger diameter (35−45 nm). The EDXS results confirm that the supported particles are NiO (Table 6). A simple

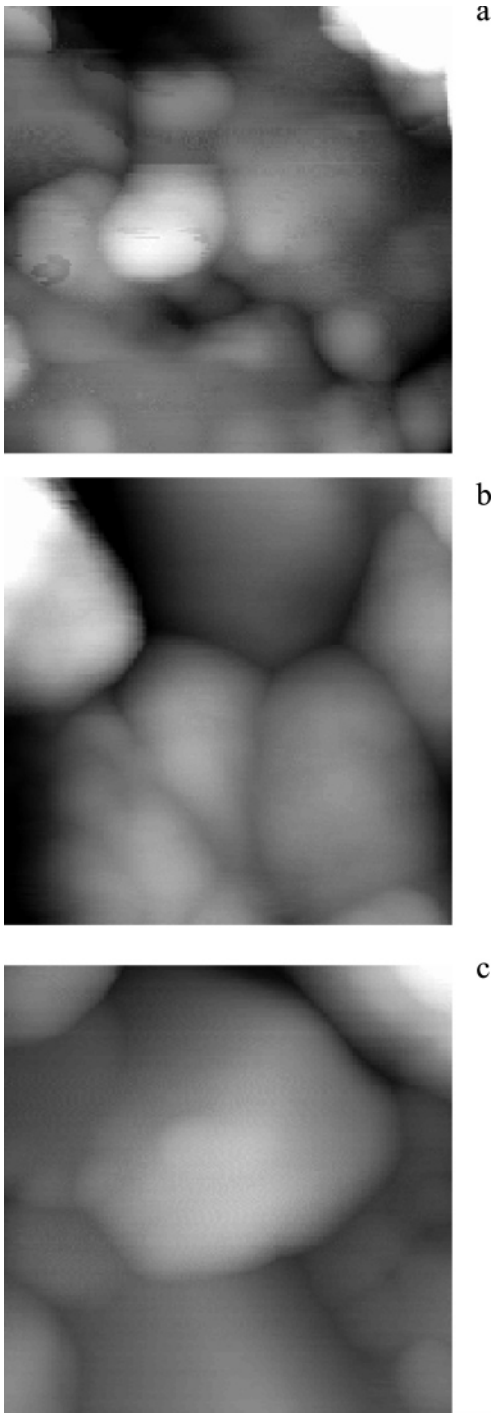

Figure 6. AFM images 0.3 × 0.3 μm^2 of the nanocomposite oxides: (a) Fe_2O_3/Co_3O_4 (Fe/Co nominal atomic ratio 0.05); (b) NiO/Co_3O_4 (Ni/Co nominal atomic ratio 0.05); and (c) NiO/Co_3O_4 (Ni/Co nominal atomic ratio 0.1).

explanation of the different growth mechanisms observed for the Fe_2O_3/Co_3O_4 and the NiO/Co_3O_4 supported oxide samples can be formulated in terms of surface energy criteria. If the support has a surface energy γ_A, the supported oxide has a surface energy γ_B, and the interface between the two has a surface energy γ_I, then the condition $\gamma_B + \gamma_I < \gamma_A$ will favor the spreading of the supported oxide on the support, whereas $\gamma_B + \gamma_I > \gamma_A$ will favor a nonwetting growth. Iron oxide tends to wet the Co_3O_4 surface giving rise to small-dimension clusters, whereas NiO forms tridimensional islands whose dimensions grow with the Ni/Co nominal

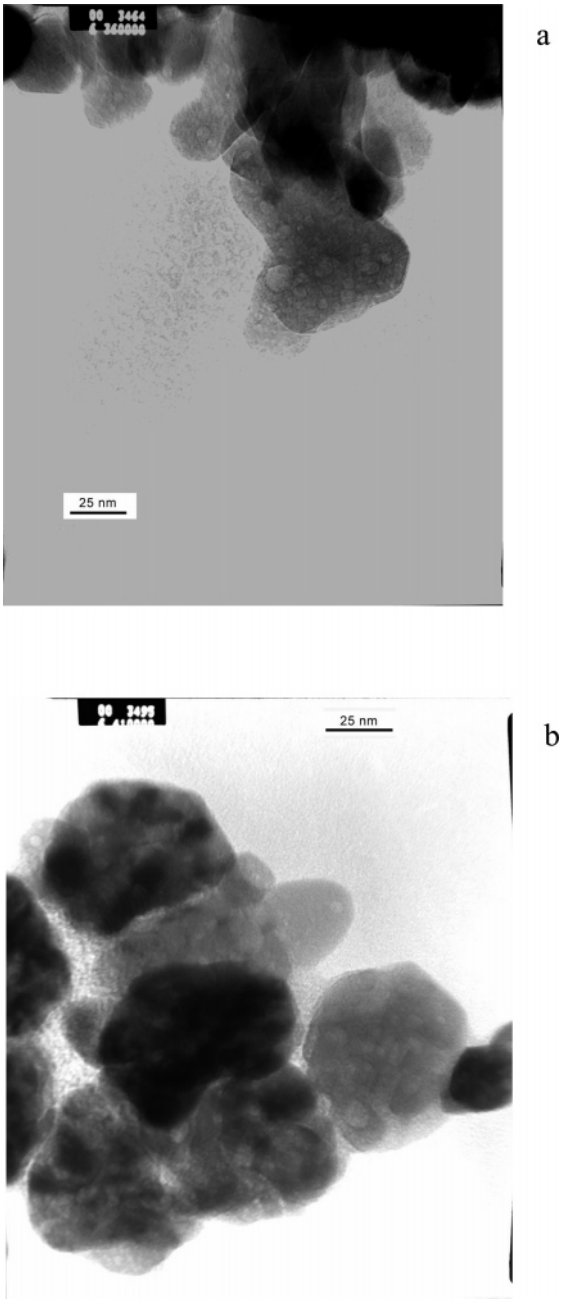

Figure 7. TEM image of the Fe_2O_3/Co_3O_4 nanocomposite oxides: (a) sample characterized by Fe/Co nominal atomic ratio 0.05; and (b) sample characterized by Fe/Co nominal atomic ratio 0.25.

Table 5. Nominal and Observed (EDXS) Atomic Composition of Fe_2O_3/Co_3O_4 Supported Oxides

nominal Fe/Co atomic ratio	observed area	O	Fe	Co
0.05	supported oxide	58	1	41
0.25	supported oxide	58	6	37

atomic ratio. It can be significant that both Fe_3O_4 and Co_3O_4 grow with spinel structure.[21] Besides the crystallographic structure, other important parameters have to be considered. Surface diffusion coefficients, for example, can play an important role; consequently the deposition temperature, as well as the preparation procedure, can influence the growing mode.

(21) Greenwood, N. N.; Earnshoow, A. *Chemistry of the Elements*; Pergamon Press: London, 1984.

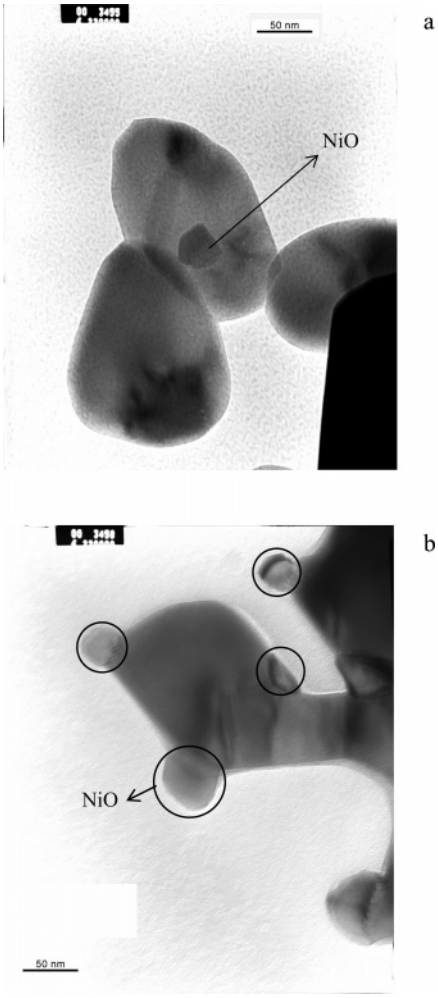

Figure 8. TEM image of the NiO/Co_3O_4 nanocomposite oxides: (a) sample characterized by Ni/Co nominal atomic ratio 0.05; and (b) sample characterized by Ni/Co nominal atomic ratio 0.1.

Table 6. Nominal and Observed (EDXS) Atomic Composition of NiO/Co_3O_4 Supported Oxides

nominal Ni/Co atomic ratio	observed area	O	Ni	Co
0.05	supported oxide	56	11	33
	supporting oxide	57	2	41
0.1	supported oxide	54	39	6
	supported oxide	59	34	6
	supporting oxide	57	3	40
	interface	68	19	13

(b) Adsorption of Pyridine. *Fe_2O_3/Co_3O_4.* The DRIFT spectra obtained after exposing the "as prepared" Fe_2O_3/Co_3O_4 powder to a pyridine/N_2 mixture at RT (Figure 9a) agree (see Table 7) with the presence of H-bonded pyridine (1589 cm^{-1})[22,23] and of pyridine interacting with Lewis (1603, 1621, and 1630 cm^{-1}),[6,24−26] and Brønsted (1639 and 1654 cm^{-1})[27,28] acidic sites. A

(22) Morterra, C.; Chiorino, A.; Ghiotti, G.; Garrone, E. *J. Chem. Soc., Faraday Trans.* **1979**, *75*, 271.
(23) Rochester, C. H.; Topham, S. A. *J. Chem. Soc., Faraday Trans.* **1979**, *75*, 1259.
(24) Knözinger, H.; Stolz, H. *Fortschr. Kolloid. Polymer* **1971**, *55*, 16.
(25) Stolz, H.; Knözinger, H. *Kolloid-Z. B* **1971**, *243*, 71.
(26) Tanabe, K. In *Catalysis−Science and Technology*; Anderson, J. R., Boudart, M., Eds.; Springer-Verlag: New York, 1981; Vol. 2, Chapter 5.
(27) Busca, G. *Catal. Today* **1998**, *41*, 191.

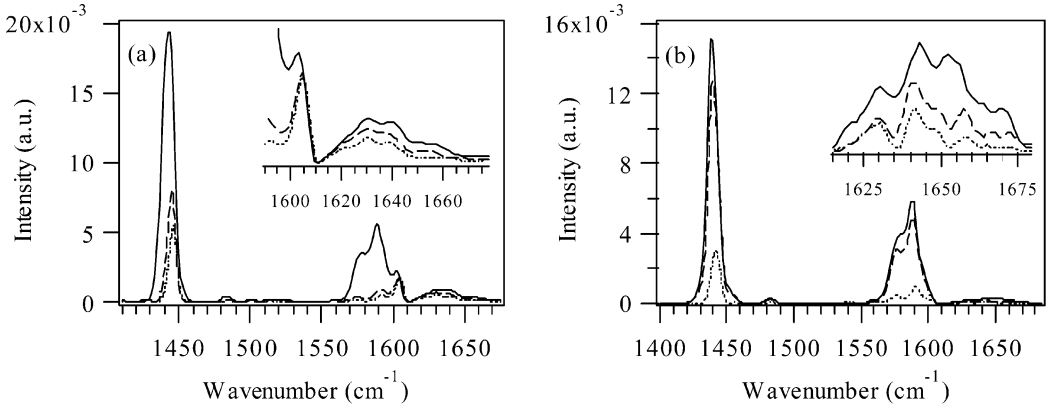

Figure 9. DRIFT spectra obtained after exposure of the Fe_2O_3/Co_3O_4 powder to the pyridine/N_2 mixture at RT (−) and successively to N_2 for 5 min (- - -) and for 30 min (···): (a) "as prepared" and (b) "pyridine-modified" Fe_2O_3/Co_3O_4.

Table 7. FTIR Data (cm^{-1}) of Liquid and Adsorbed Pyridine (vs, very strong; s, strong; m, medium; w, weak; v, variable)

	liquid and/or physisorbed py[a]	H-bound py[b,c]	Lewis py[b,c]	Brønsted py[b,c]
8a	1583 vs	1580−1600 s	1600−1633 s	∼1640
8b	1572 m		∼1580 v	1608
19a	1482	1485−1490 w	1488−1503 v	1535−1540 s
19b	1432−1441	1440−1447 vs	1447−1460 v	1485−1500 vs

[a] Ref 30. [b] Ref 28. [c] Ref 32.

broad band at about 3100−3700 cm^{-1} (i.e., in the spectral region characteristic of the O−H stretching vibrations) suggests that the interaction with pyridine perturbs the OH groups.[23,29]

In the DRIFT spectra obtained upon exposure of the "pyridine-modified" surface to the pyridine/N_2 mixture at RT (Figure 9b) liquidlike and H-bonded pyridine are prevalent, as pointed out by the signals of the 8a, 19a, and 19b ring-stretching modes centered at 1589, 1580, 1482, and 1439 cm^{-1}.[23,30−32] Inspection of Figure 9b reveals the presence of Lewis (1630 cm^{-1}) and Brønsted (1643 and 1655−1660 cm^{-1}) acidic sites.

After evacuation at RT H-bonded and liquidlike pyridine rapidly disappear, whereas the pyridine molecules interacting with Lewis and Brønsted acid centers are still evident (Figure 9a and b). As far as the strength of the Lewis and Brønsted acidic sites is concerned, the position of contribution of the peak 8a (Figure 9) upon adsorption suggests the presence of medium- to high-strength acidic sites (Table 7).[27,33]

NiO/Co_3O_4. The DRIFT spectra obtained upon exposing the "as-prepared" and "pyridine modified" NiO/Co_3O_4 nanocomposite mixed oxide to pyridine at RT do not show significant differences. In Figure 10 the DRIFT spectra obtained upon exposure of the "as-prepared" surface to the pyridine/N_2 mixture and successively to N_2 at RT are shown. Very weak signals agree with the presence of liquidlike pyridine (1433, 1441, 1450, and

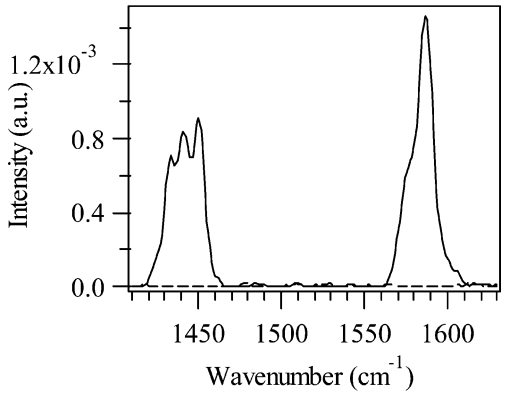

Figure 10. DRIFT spectra obtained after exposure of the NiO/Co_3O_4 powder to the pyridine/N_2 mixture at RT (−) and successively to N_2 for 5 min (- - -).

1587 cm^{-1}) and Lewis acidic sites (weak shoulder at 1606 cm^{-1}). Significantly, pyridine is completely removed from the surface by N_2 (Figure 10) confirming the weakness of the interaction (and thus the low strength of the acidic sites) at variance to the Fe_2O_3/Co_3O_4 system.

Co_3O_4. The "as-prepared" Co_3O_4 was also exposed to pyridine for comparison. The observed signals (Figure 11a) agree with the presence of pyridine H-bonded to the surface (1591 cm^{-1})[29,31] and interacting with Lewis acidic sites (1603 cm^{-1}).[34] The latest contribution becomes more evident after evacuation. The OH groups are perturbed by the adsorption of pyridine as confirmed by a broad band at about 3400 cm^{-1} (Figure 11b).[29,31]

Summarizing, the interaction with pyridine demonstrates the presence of both Lewis (1606 cm^{-1}) and Brønsted (1639 cm^{-1}) acidic sites on the iron oxide surface.[35] The comparison of the results obtained on the pure and supported oxides suggests the formation of new Lewis and Brønsted acidic sites as a consequence of the interaction between the two oxides in the Fe_2O_3/Co_3O_4 nanocomposite material; pyridine interacts with these sites giving rise to the signals at 1630, 1621 (Lewis), and 1654 cm^{-1} (Brønsted). In the NiO/Co_3O_4 sample, in contrast, no new sites were observed; moreover, the rather weak Lewis acidic sites observed on the Co_3O_4 surface (whose interaction with pyridine gives

(28) Parry, E. P. *J. Catal.* **1963**, *2*, 371.
(29) Morterra, C.; Ghiotti, G.; Boccuzzi, F.; Coluccia, S. *J. Catal.* **1978**, *51*, 299.
(30) Corrsin, L.; Fax, B. J.; Lord, R. C. *J. Chem. Phys.* **1953**, *21*, 1170.
(31) Morterra, C.; Ghiotti, G.; Garrone, E.; Fisicaro, E. *J. Chem. Soc., Faraday Trans. 1* **1980**, *76*, 2101.
(32) Morterra, C.; Chiorino, A.; Ghiotti, G.; Fisicaro, E. *J. Chem. Soc., Faraday Trans. 1* **1982**, *78*, 2649.
(33) Lorenzelli, V.; Busca, G.; Sheppard, N. *J. Catal.* **1980**, *66*, 28.
(34) Miyata, H.; Nakagawa, Y.; Ono, T.; Kubokawa, Y. *J. Chem. Soc., Faraday Trans. 1* **1983**, *79*, 2343.
(35) Ferretto, L.; Glisenti, A. *J. Mol. Catal. A* **2002**, *187*, 119.

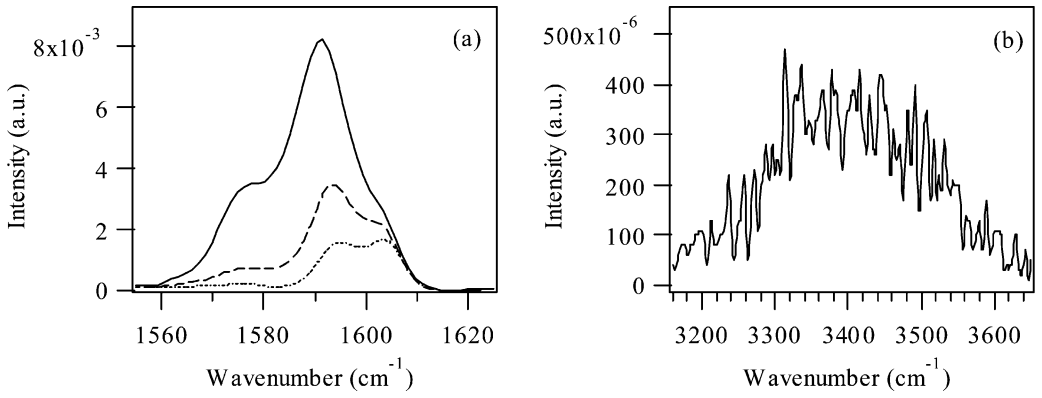

Figure 11. DRIFT spectra obtained after exposure of the Co_3O_4 powder to the pyridine/N_2 mixture at RT (−) and successively to N_2 for 5 min (- - -) and for 30 min (···); (a) spectral region from 1555 to 1625 cm^{-1}, and (b) spectral region from 3160 to 3650 cm^{-1}.

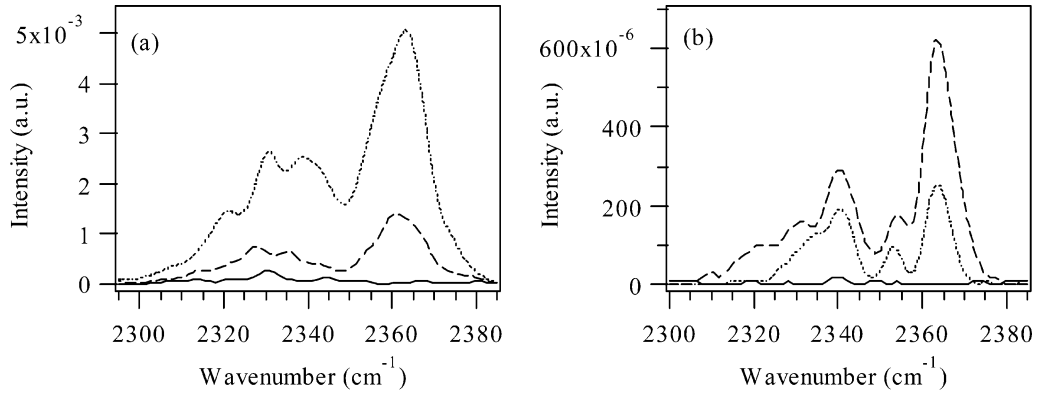

Figure 12. DRIFT spectra obtained after the exposure of "as-prepared" (a) Fe_2O_3/Co_3O_4 and (b) Co_3O_4 samples to the pyridine/N_2 mixture at RT (−) and successively to N_2 for 5 min (- - -) and for 30 min (···): region characteristic of the asymmetric stretching vibrations of CO_2.

Scheme 1

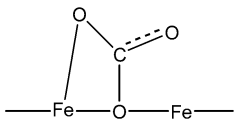

rise to the signal at 1603 cm^{-1}) are not significant on the NiO/Co_3O_4 nanocomposite catalyst.

An interesting result derives from the observation of the reactivity as a function of time. The DRIFT spectra (Figure 12) clearly indicate the formation of CO_2 both on Fe_2O_3/Co_3O_4 and Co_3O_4 and thus a high reactivity toward oxidation due to the reactive sites distributed on the Co_3O_4 surface. Only the DRIFT spectra collected after a short reaction time were thus considered to investigate the acidic sites.

(c) Adsorption of Carbon Dioxide. The spectra obtained upon exposure of the Fe_2O_3/Co_3O_4 nanocomposite oxide to CO_2 (Figure 13a and b) reveal a weak interaction: traces of unicoordinated carbonates are evidenced by a very weak signal around 1418 cm^{-1} which shifts at slightly lower wavenumbers (1405 cm^{-1}) if the adsorption is carried out at 373 K.[36−38] In both cases the carbonates are completely removed by the nitrogen flow confirming that the basic sites are very weak. In the spectral region characteristic of the asymmetric stretching of CO_2 (Figure 13a) several peaks can be observed (2360, 2341, 2331, 2324, and 2313 cm^{-1}). Careful comparison with the spectrum of gas-phase carbon dioxide suggests a weak interaction between CO_2 and the cations distributed on the nanocomposite oxide surface. Consistently, traces of signals are still observed in this region after exposure to N_2. Similar results are obtained upon exposure to CO_2 at 373 K.

Several signals (2367, 2356, 2344, 2332, 2328, 2322, and 2314 cm^{-1}) are evident on the DRIFT spectrum observed after exposing the NiO/Co_3O_4 mixed oxide to CO_2 (Figure 13c); their presence after evacuation indicates the interaction with the Lewis acidic sites. The adsorption experiment carried out at 373 K also reveals a few peaks (2366, 2356, 2337, 2326, and 2312 cm^{-1}) and thus the existence of carbon dioxide molecules interacting with Lewis acidic sites.

It is noteworthy that the DRIFT spectrum observed after the exposure of Co_3O_4 to CO_2 (Figure 13d) does not indicate the presence of basic sites: in fact, no carbonate species are present. Moreover, all the signals characteristic of CO_2 disappear after evacuation; this result, as well as the shape of the peak due to the C−O stretching, indicates that CO_2 does not interact with the Co_3O_4 surface. The formation of bidentate carbonate species, however, suggested the presence of complex sites constituted by a metal ion and the neighboring oxygen on the Fe_2O_3 surface (Scheme 1).[33] These sites disappear in the Fe_2O_3/Co_3O_4 nanocomposite oxide.

(36) Gatehouse, B. M.; Livingstone, S. E.; Nyholm, R. S. *J. Chem. Soc.* **1958**, 3137.
(37) Little, L. H. In *Infrared Spectra of Adsorbed Species*; Academic Press: San Diego, CA, 1966; Chapter 3.
(38) Auroux, A.; Gervasini, A. *J. Phys. Chem.* **1990**, *94*, 6371.

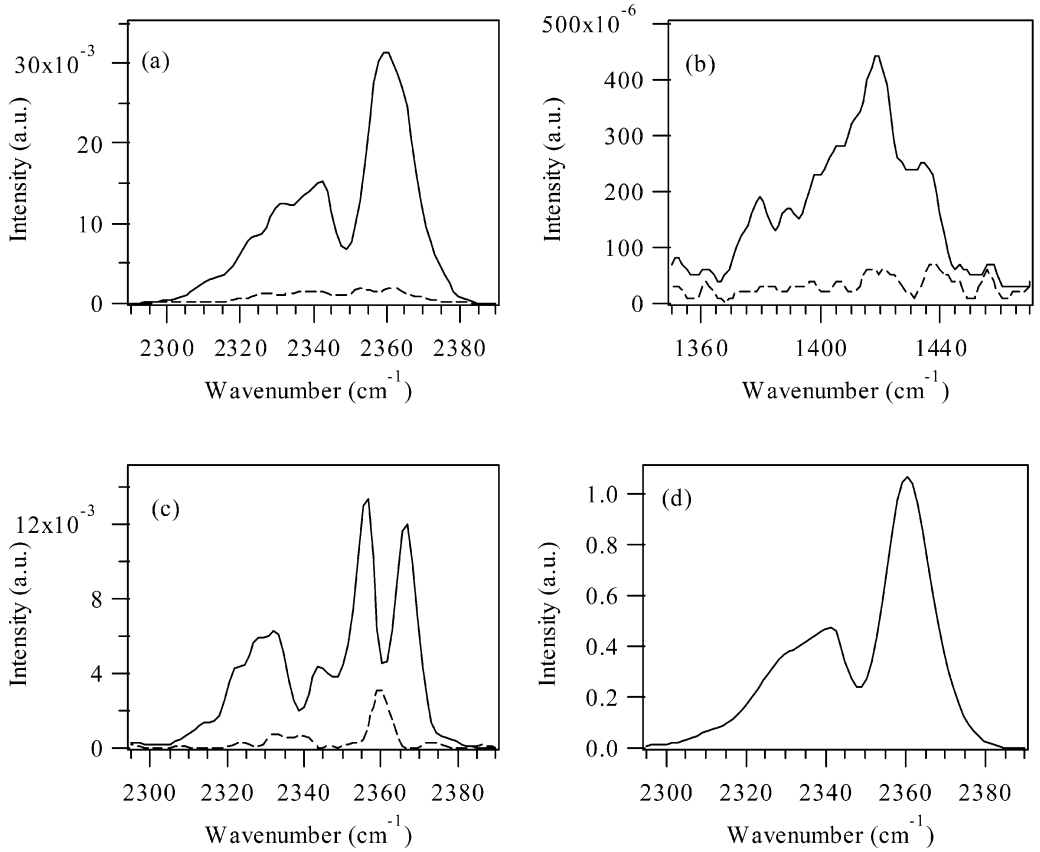

Figure 13. DRIFT spectra obtained after exposure of the Fe_2O_3/Co_3O_4 and NiO/Co_3O_4 powder samples to CO_2 at RT (—) and successively to N_2 for 5 min (- - -). (a) Fe_2O_3/Co_3O_4: spectral region from 2290 to 2390 cm^{-1}; (b) Fe_2O_3/Co_3O_4: spectral region from 1350 to 1470 cm^{-1}; (c) NiO/Co_3O_4: spectral region from 2260 to 2420 cm^{-1}; (d) spectrum obtained upon exposure of Co_3O_4 to CO_2 at RT.

Conclusions

In this paper investigation of two supported oxides (NiO/Co_3O_4 and Fe_2O_3/Co_3O_4) is reported. The supported oxides were obtained by wet impregnation followed by heating treatments; several supported oxides characterized by different compositions (different Ni/Co and Fe/Co atomic ratios) were prepared and a submonolayer composition (Ni/Co, 0.1 and Fe/Co, 0.1) was chosen for a deeper investigation. A careful characterization of the prepared samples was carried out by means of XP and DRIFT spectroscopic techniques, XRD, thermal analysis, AFM, and TEM. Moreover, the acidic and basic sites distributed on the nanocomposite oxide surfaces were studied by means of their interaction with test molecules (pyridine and carbon dioxide).

(1) The growing mode on cobalt oxide is different for iron and nickel oxide. Iron oxide wets the surface, and small particles (ca. 5 nm) homogeneously distribute on the support. In contrast, bigger islands of NiO (35−45 nm) grow on the cobalt oxide surface.

(2) Thermal analysis, XP, and DRIFT spectroscopic techniques indicate a significant decrease of the hydroxyl groups as a consequence of the deposition of iron and nickel oxide on cobalt oxide. This result suggests the interaction of supported and supporting oxides by means of a condensation mechanism. The grafting of supporting and supported oxide by hydroxyl condensation determines the formation of Co−O−M (M = Fe or Ni) sites.

(3) The presence of the Fe_2O_3 oxide seems to influence the stability of the Co_3O_4 with respect to its reduction to CoO.

(4) New acidic sites were observed on the Fe_2O_3/Co_3O_4 sample surface, whereas this result was not evident for NiO/Co_3O_4. The complex sites constituted by an Fe (III) cation and its neighboring oxygen atom were observed on hematite but disappear in the Fe_2O_3/Co_3O_4 mixed oxide.

Acknowledgment. We gratefully acknowledge Professor E. Tondello for helpful discussions, Professor P. Colombo for the XRD measures, and Dr. S. Gialanella for the TEM measurements.

CM031019E